Facilitation of Calmodulin-Mediated Odor Adaptation by cAMP-Gated Channel Subunits

Jonathan Bradley,[1,2]* Dirk Reuter,[1]† Stephan Frings[1]‡

Calcium (Ca^{2+}) influx through Ca^{2+}-permeable ion channels plays a pivotal role in a variety of neuronal signaling processes, and negative-feedback control of this influx by Ca^{2+} itself is often equally important for modulation of such signaling. Negative modulation by Ca^{2+} through calmodulin (CaM) on cyclic nucleotide–gated (CNG) channels underlies the adaptation of olfactory receptor neurons to odorants. We show that this feedback requires two additional subunits of the native olfactory channel, CNGA4 and CNGB1b, even though the machinery for CaM binding and modulation is present in the principal subunit CNGA2. This provides a rationale for the presence of three distinct subunits in the native olfactory channel and underscores the subtle link between the molecular make-up of an ion channel and the physiological function it subserves.

Vertebrate olfactory signal transduction involves activation of specific neuronal heterotrimeric GTP-binding protein (G protein)–coupled receptors by odorant molecules. This in turn stimulates adenylyl cyclase, and the resulting increase in intracellular adenosine 3′,5′-monophosphate (cAMP) concentration causes CNG channels (*1*) to open and the olfactory receptor neuron (ORN) to depolarize to firing threshold (*2*). Olfactory CNG channels have a substantial Ca^{2+} permeability (*3*), which triggers adaptation of ORNs (*4–6*). One major component of this adaptation is thought to involve negative modulation of CNG channels by Ca^{2+}/calmodulin (Ca^{2+}-CaM) association (*5–8*). The native olfactory CNG channel is a heteromeric complex of a principal subunit, CNGA2, and two modulatory subunits, CNGA4 and CNGB1b (neither of which forms functional CNG channels by itself, but each of which increases the sensitivity of CNGA2 to cAMP) (*9–12*). In whole-cell recording experiments on ORNs, the negative-feedback modulation of the channel by Ca^{2+} is fast, reaching a steady state in less than 500 ms (*5*). However, inside-out membrane patch recording experiments on heterologously expressed homomeric CNGA2 channels have shown that feedback inhibition is much slower (*13*), suggesting the possible influence of modulatory CNG subunits on channel inhibition by Ca^{2+}-CaM.

To examine the response of native CNG channels in rat ORNs to cAMP, we used flash photolysis of caged cAMP that was introduced into the cell (*14*) (Fig. 1A). The current that was activated by photoreleased cAMP rapidly declined to base line within ~500 ms, regardless of whether the activated current was small or near saturation (Fig. 1A). Current decay was not observed in the absence of extracellular Ca^{2+} (Fig. 1A, inset), indicating that it depended on Ca^{2+} influx. In contrast, homomeric CNGA2 channels expressed in human embryonic kidney (HEK) 293 cells (*14*) produced a current that declined about 100 times more slowly (Fig. 1B). In excised membrane patches (taken from the same HEK 293 cells before and after the Ca^{2+}-dependent current decline), there was a shift in the steady-state dose-response relation between current activation and cyclic nucleotide concentration, and this shift was reproduced with CaM (Fig. 1C) (*15*). Despite the shift in the dose-response relation, the maximum current remained unchanged, suggesting that the single-channel current would also remain unchanged. Consistent with previous results (*7*), direct single-channel recording (*16*) confirmed that Ca^{2+}-CaM decreased the open probability (P_o) of the channel without affecting its conductance. These data suggest that binding of Ca^{2+}-CaM suppresses the current by reducing P_o, and that this inhibition can be overcome with a higher ligand concentration. Thus, in the steady state, when Ca^{2+}-CaM is bound to the CNG channel, it likely influences the gating process (*17*). Taken together, these data show that the decline of the cyclic nucleotide–activated current under whole-cell conditions is the consequence of a Ca^{2+}-CaM–mediated decline of the channels' ligand sensitivity, which causes a reduction of P_o at submaximal ligand concentrations.

The kinetic difference in current decline between native and CNGA2 channels could be attributed to effects of the modulatory subunits on the mechanics of the Ca^{2+}-CaM modulation. To examine this possibility, we expressed the three CNG subunits in all combinations and, for each combina-

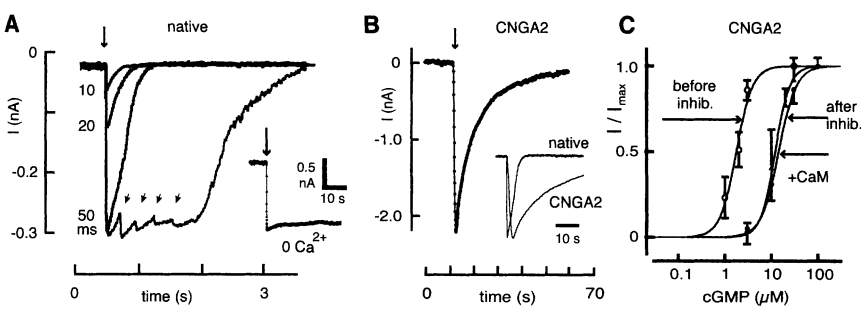

Fig. 1. Ca^{2+}-CaM inhibits olfactory CNG channels in the whole-cell configuration. (**A**) Transient activation of CNG channels in an isolated rat ORN by photolysis of caged cAMP (*14*). The whole-cell inward current (*I*) at −50 mV is shown during photolysing light flashes of 10, 20, or 50 ms (arrow). The 50-ms flash induced maximal channel activation, because four additional 50-ms flashes (arrowheads) prolonged the CNG current but did not increase its amplitude. In Ca^{2+}-free bath solution, a 50-ms flash induced a larger and sustained current (inset), reflecting relief of blockage by Ca^{2+} and lack of Ca^{2+}-dependent inhibition. (**B**) Current transient induced by photolysis of 8-Br-cGMP at −70 mV in an HEK 293 cell expressing rat CNGA2 (*14*). (Inset) The difference in time course of inhibition between native and CNGA2 channels. (**C**) Macroscopic dose-response relations for CNGA2 channel activation by cGMP (*15*) show that the current declines in the whole-cell recordings were caused by Ca^{2+}-CaM. cGMP sensitivity of CNGA2 channels is high before the photolysis experiment in (B) (before inhibition: $K_{1/2}$ = 1.7 ± 0.3 μM, n = 2.5 ± 0.9) and reduced after complete decay of the photolysis-induced current (after inhibition: $K_{1/2}$ = 14.3 ± 2.9 μM, n = 2.3 ± 0.3). This increase in $K_{1/2}$ was reproduced in the same patches by Ca^{2+}-CaM (+CaM; $K_{1/2}$ = 12.0 ± 2.8 μM, n = 2.8 ± 0.3). Values (mean ± SD) are from seven cells.

[1]Institut für Biologische Informationsverarbeitung, Forschungszentrum Jülich, 52425 Jülich, Germany. [2]Laboratoire de Neurobiologie, Ecole Normale Supérieure, 75230 Paris, France.

*Present address: Howard Hughes Medical Institute, Department of Neuroscience, Johns Hopkins University School of Medicine, Baltimore, MD 21205, USA.
†Present address: Sophion Bioscience, Pederstrupvej 93, 2750 Ballerup, Denmark.
‡To whom correspondence should be addressed. E-mail: s.frings@fz-juelich.de

tion, recorded the kinetics of Ca^{2+}-CaM–mediated inhibition in excised inside-out patches (*18*). Homomeric CNGA2 channels responded much more slowly to the application of 1 μM CaM than native channels or channels containing all three subunits (CNGA2A4B1b) (Fig. 2A), consistent with the whole-cell result (Fig. 1). CNGA2 channels also recovered more rapidly when Ca^{2+}-CaM was removed. Overall, there was not much difference in inhibition rate with CNGA2 alone or in combination with either CNGA4 or CNGB1b. However, coassembly of all three subunits resulted in a rapid inhibition by Ca^{2+}-CaM (Fig. 2B) that was comparable to that of the native channel.

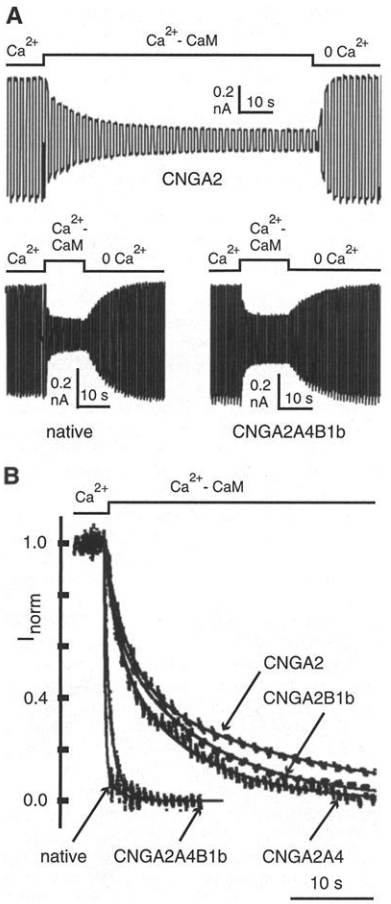

Fig. 2. The rate of Ca^{2+}-CaM–induced current decline is determined by channel subunit composition. (**A**) Homomeric CNGA2 channels (top) displayed slower decline and faster recovery than native channels (bottom left) and CNGA2A4B1b channels (bottom right). Inside-out recordings were made during alternating voltage pulses (±40 mV) with 100 μM cAMP (CNGA2) or 10 μM cAMP (native and CNGA2A4B1b), resulting in a mean initial P_o before CaM application of 0.7 to 0.9 (*23*). Current declined in response to application of 150 μM Ca^{2+} and 1 μM CaM, and recovered upon CaM removal in Ca^{2+}-free solution. (**B**) Time course of inhibition of native channels and of channels with the indicated subunit compositions during exposure to 150 μM Ca^{2+} and 1 μM CaM. Currents recorded at an initial P_o of 0.7 to 0.9 were normalized to the amplitude of the CaM response (*19*).

The slower rate of current decline in the absence of the modulatory subunits could have resulted from a slower rate of Ca^{2+}-CaM binding or from a slower response of the channel after Ca^{2+}-CaM association. To test these possibilities, we performed a CaM pulse experiment. For homomeric CNGA2 channels, a prolonged, 100-s pulse of CaM in the continuous presence of excess Ca^{2+} produced slow inhibition of the cGMP-induced current (Fig. 3A). Shorter pulses also produced current decline but during the Ca^{2+}-CaM pulse only; current stopped at the removal of CaM and stayed approximately constant in the continuous presence of excess Ca^{2+}. This indicated that CaM binding is rate-limiting for the development of inhibition. Furthermore, the sustained inhibition upon removal of CaM at constant Ca^{2+} shows that dissociation of Ca^{2+}-CaM from the channel is much slower than association. Assuming that this dissociation is infinitely slow, the on-rate of Ca^{2+}-CaM becomes simply proportional to the reciprocal of the time constant of current decline (*19*). From such measurements on CNGA2 and CNGA2A4B1b channels (for which the dissociation is likewise slow) (*20*) at different CaM concentrations (Fig. 3, B and C), the rate constant for fast Ca^{2+}-CaM association with the channels, k_f, could be obtained (Fig. 3D) (*19*, *21*). We derived k_f values of 6.7×10^4 M^{-1} s^{-1} for CNGA2 channels and 1.7×10^7 M^{-1} s^{-1} for CNGA2A4B1b channels, representing a >200-fold difference in on-rate. Accordingly, the inhibition time course of CNGA2 channels at 900 nM CaM matched fairly well that of CNGA2A4B1b channels at 2 nM CaM (Fig. 3C).

What is the mechanism underlying the slow kinetics of Ca^{2+}-CaM association to homomeric CNGA2 channels? One possibility is that the association depends on whether the channel is in the open or closed state (*22*). To address this possible state dependence, we measured the time course of current decline during application of Ca^{2+}-CaM at various concentrations of cGMP, i.e., at different initial levels of P_o. The rate of CaM binding to homomeric CNGA2 channels depended on the P_o of channels before CaM was applied (mean initial P_o) (*23*) (Fig. 4A). In contrast, for CNGA2A4B1b channels, the time course of current inhibition showed no such P_o dependence (Fig. 4B). For CNGA2 channels, k_f decreased >10-fold when P_o was increased from near 0 to 1 (Fig. 4C). However, CNGA2A4B1b channels showed no decrease in k_f over the entire P_o range. Furthermore, even at a P_o near zero (when the channel is in the closed state), the k_f of Ca^{2+}-CaM for CNGA2A4B1b channels

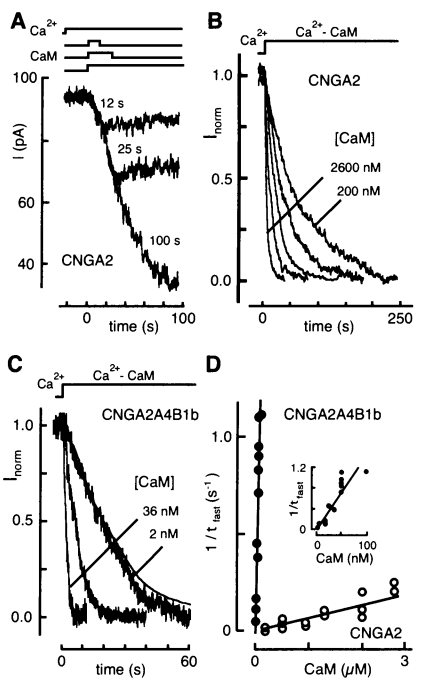

Fig. 3. Modulatory subunits increase rate of Ca^{2+}-CaM association with channels. (**A**) CaM association is the rate-limiting step for current decline. Three superimposed current recordings were made at 300 μM Ca^{2+} and 5 μM cGMP from an inside-out membrane patch with CNGA2 channels that were challenged successively with 500 nM CaM for periods of 12, 25, and 100 s. Between recordings, CaM was washed off the patch in Ca^{2+}-free solution. Inhibition freezes upon removal of CaM from the patch (at constant Ca^{2+} concentration), demonstrating that the Ca^{2+}-CaM association step is rate-limiting for current decline. Current recovery in the absence of bath CaM (at constant Ca^{2+}) is much slower than association. (**B**) Dependence of the rate of current decline on CaM concentration with CNGA2 channels. Five recordings from the same patch were made at +40 mV with 5 μM cGMP and 300 μM Ca^{2+} during application of 2600, 1300, 900, 500, and 200 nM CaM (from left). (**C**) Dependence of the rate of current decline on CaM concentration with CNGA2A4B1b channels. Current recordings were made at +40 mV with 3 μM cGMP and 50 μM Ca^{2+} during application of 36, 18, and 2 nM CaM (from left). The time course of CNGA2A4B1b channel inhibition at 2 nM CaM corresponds to the time course of CNGA2 channel inhibition at 900 nM (smooth line). (**D**) Determination of rate constants for fast Ca^{2+}-CaM association with the channels (k_f) from the fast time constant of inhibition ($1/\tau_{fast} = k_f[CaM]$) (*19*) yields 6.7×10^4 M^{-1} s^{-1} for CNGA2 channels and 1.7×10^7 M^{-1} s^{-1} for CNGA2A4B1b channels. (Inset) The CNGA2A4B1b data on an extended scale of CaM concentrations.

was at least 10-fold higher than for CNGA2 channels.

For the negative-feedback modulation by Ca^{2+}-CaM to produce rapid adaptation of the ORN at strong odor stimulation, Ca^{2+}-CaM must bind effectively to the open state of the CNG channel. Because Ca^{2+}-CaM binds better to a closed rather than open homomeric CNGA2 channel, its inhibitory effect upon binding would be of little use during odorant stimulation. We find that only in the presence of CNGA4 and CNGB1b, the two modulatory CNG subunits of the olfactory CNG channel, can Ca^{2+}-CaM bind rapidly to the open state. In rod phototransduction, a negative feedback by Ca^{2+}-CaM on the CNG channel likewise exists, with preferred binding to the closed rod channel (*24*). However, in contrast to olfactory CNG channels in ORNs, rod CNG channels in photoreceptor cells always operate at very low levels of P_o (*25*), so that state dependence of Ca^{2+}-CaM binding to the closed channel would not compromise the feedback inhibition. Because CNG channels mediating visual transduction in retinal rod photoreceptors are composed of CNGA1 (*1*), a homologous principal subunit to olfactory CNGA2, and CNGB1a, an alternatively spliced form of the olfactory CNGB1b subunit, we conclude that the CNGA4 subunit contributes a specific function for olfactory adaptation. In ORNs, where CNG channels reach high levels of P_o, the CNGA4 subunit facilitates Ca^{2+}-CaM binding to open channels and, hence, transforms the negative feedback by Ca^{2+}-CaM into the rapid and state-independent control mechanism that is needed for olfactory adaptation

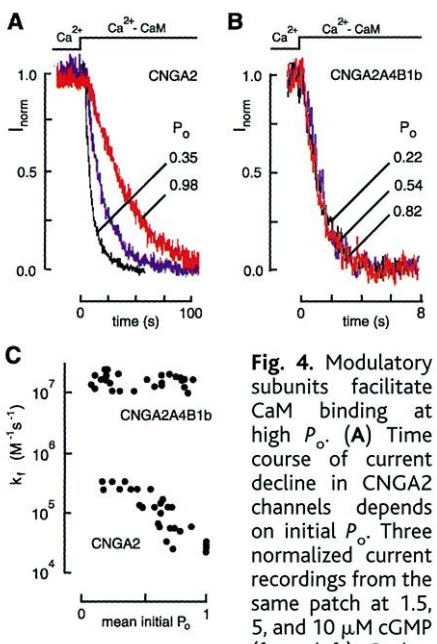

Fig. 4. Modulatory subunits facilitate CaM binding at high P_o. (**A**) Time course of current decline in CNGA2 channels depends on initial P_o. Three normalized current recordings from the same patch at 1.5, 5, and 10 μM cGMP (from left). P_o before addition of 500 nM CaM was 0.35, 0.88, and 0.98, respectively. (**B**) Time course of current decline in CNGA2A4B1b channels did not depend on initial P_o. Three recordings are shown at 0.9, 2, and 3 μM cGMP during application of 50 nM CaM (50 μM Ca^{2+}). Initial P_o was 0.22, 0.54 and 0.82, respectively, and no significant difference in τ_{fast} (1.2 to 1.3 s) was detected. (**C**) Rate constant of fast Ca^{2+}-CaM association, k_f, changes markedly with P_o for CNGA2 channels but shows no P_o dependence in CNGA2A4B1b channels.

References and Notes

1. Different nomenclature has been under consideration in the field, and we and Munger *et al.* (*26*) have used a common nomenclature based on an informal survey of 20 colleagues in the field. Our discussion and proposal is described in a Letter in this issue (www.sciencemag.org/cgi/content/summary/294/5549/2093a).
2. S. Frings, *Cell. Mol. Life Sci.* **58**, 510 (2001).
3. C. Dzeja, V. Hagen, U. B. Kaupp, S. Frings, *EMBO J.* **18**, 131 (1999).
4. T. Kurahashi, *J. Physiol.* **430**, 355 (1990).
5. _____, A. Menini, *Nature* **385**, 725 (1997).
6. F. Zufall, T. Leinders-Zufall, *Chem. Senses* **25**, 473 (2000)
7. T. Y. Chen, K. W. Yau, *Nature* **368**, 545 (1994).
8. M. D. Varnum, W. N. Zagotta, *Science* **278**, 110 (1997).
9. A. Sautter, X. Zong, F. Hofmann, M. Biel, *Proc. Natl. Acad. Sci. U.S.A.* **95**, 4696 (1998).
10. W. Bönigk *et al.*, *J. Neurosci.* **19**, 5332 (1999).
11. J. Bradley, J. Li, N. Davidson, H. A. Lester, K. Zinn, *Proc. Natl. Acad. Sci. U.S.A.* **91**, 8890 (1994).
12. E. R. Liman, L. B. Buck, *Neuron* **13**, 611 (1994).
13. M. Liu, T. Y. Chen, B. Ahamed, J. Li, K. W. Yau, *Science* **266**, 1348 (1994).
14. ORNs were isolated from rat olfactory epithelium (*27*) and maintained in a solution containing (mM) 55 NaCl, 70 methanesulfonic acid, 2 $CaCl_2$, 1 $MgCl_2$, 0.25 niflumic acid, 10 Hepes (pH 7.4, *N*-methyl-D-glucamine). The pipette solution for whole-cell experiments contained (mM) 8 CsCl, 117 methanesulfonic acid, 0.5 EGTA, 10 Hepes (pH 7.2, CsOH), and 100 μM [6,7-*bis*(carboxymethoxy)coumarin-4-yl] methyl (BCMCM)–caged cAMP (*28*). Recordings were made at chloride equilibrium potential (−50 mV) with niflumic acid in the bath to suppress Ca^{2+}-activated Cl^- currents. Photorelease of cAMP was triggered by ultraviolet flashes (330 to 400 nm). Between flashes, recovery intervals of 3 min allowed hydrolysis of cAMP. In whole-cell recordings with HEK 293 cells, the bath solution contained (mM) 140 NaCl, 5 KCl, 0.3 $CaCl_2$, 50 glucose, 10 Hepes (pH 7.4, NaOH). The pipette solution contained (mM) 130 CsCl, 10 NaCl, 0.5 EGTA, 10 Hepes (pH 7.2, CsOH), and 5 μM 4,5-dimethoxy-2-nitrobenzyl (DMNB)–caged 8-Br-cGMP. 8-Br-cGMP is an efficient activator of CNGA2 channels with a concentration for half-maximal activation, $K_{1/2}$, of 0.15 μM (*29*). Olfactory CNGs can be activated by cGMP and by cAMP. For all subunit compositions, the $K_{1/2}$ values are near 1.8 μM for cGMP (*9*). $K_{1/2}$ values for cAMP are as follows: CNGA2, 45 μM; CNGA2B1b, 30 μM; CNGA2A4, 10 μM; CNGA2A4B1b, 4.8 μM; native channels, 4.1 μM (*10*).
15. CNGA2 was expressed in HEK 293 cells (*10*), and the sensitivity to cGMP was measured in two inside-out patches from the same cell, taken before and after a photorelease experiment in the whole-cell configuration. For inside-out recordings, the pipette solution contained (mM) 140 NaCl, 5 KCl, 5 EGTA, 10 Hepes (pH 7.4, NaOH). Patches were excised into a solution containing (mM) 140 NaCl, 5 KCl, 0.3 $CaCl_2$, 10 Hepes (pH 7.2, NaOH). The high Ca^{2+} concentration ensured that cytosolic Ca^{2+}-binding proteins, bound to CNGs during channel activity in the cell, did not dissociate. Dose-response relations for cGMP were recorded in the same solution. The effect of CaM was studied by first washing patches in Ca^{2+}-free solution (to remove all Ca^{2+}-binding proteins), and then applying 0.5 μM bovine brain CaM (Calbiochem, Germany) with 0.3 mM Ca^{2+} for 3 min to allow CaM association with the channels. Dose-response relations were constructed by fitting to the data a Hill-type function, $I/I_{max} = c^n/(c^n + K_{1/2}^n)$, where I_{max} is the current at saturating cGMP concentration, c is the cGMP concentration, and n is the Hill coefficient. Values of I/I_{max} for each cGMP concentration are shown as the mean ± SD.
16. D. Reuter, J. Bradley, S. Frings, data not shown.
17. Detailed studies of the steady-state aspects of Ca^{2+}-CaM association with CNG channels are presented elsewhere (*7*, *13*, *16*, *30*).
18. Inside-out patches were subjected to an alternating-voltage protocol (±40 mV) for better patch stability. Patches were first washed in Ca^{2+}-free solution containing (mM) 140 NaCl, 5 KCl, 5 EGTA, 50 glucose, 10 Hepes (pH 7.2, NaOH) for 0.5 to 1 min, and then exposed to a solution containing (mM) 140 NaCl, 5 KCl, 10 Hepes (pH 7.2, NaOH) and the indicated concentrations of $CaCl_2$ and cyclic nucleotides. Current decline was started by rapidly (within <50 ms) changing to a solution containing CaM.
19. In most patches, the time course of current decline was best described by the sum of two exponentials

$$I_{norm}(t) = a_f e^{-\frac{t}{\tau_{fast}}} + (1-a_f)e^{-\frac{t}{\tau_{slow}}} \quad (1)$$

indicating that the association kinetics of Ca^{2+}-CaM and the channel is more complex than a simple one-step process. τ_{fast} and τ_{slow} describe the fast and the slow components of current decline, and a_f represents the relative contribution of the fast component. Details of the kinetic analysis and the fitting parameters are available on *Science* Online at www.sciencemag.org/cgi/content/full/294/5549/2176/DC1.
20. J. Bradley, D. Reuter, S. Frings, data not shown.
21. The two modulatory subunits also increased τ_{slow}, but the fitted values displayed substantial scatter and were excluded from further analysis (*19*). Thus, our kinetic analysis describes the initial step in current decline, the binding of Ca^{2+}-CaM to the channel. Molecular rearrangements of the channel that follow CaM binding and eventually alter channel gating are not reflected in our experimental parameter, τ_{fast}.
22. S. E. Gordon, *Methods Enzymol.* **315**, 772 (2000).
23. To calculate the mean initial P_o of channels in an excised patch before addition of CaM, we determined the macroscopic current at the given ligand concentration (I) and the maximal current at saturating ligand concentration (I_{max}). P_o is related to the maximal open probability (P_o^{max}) according to $P_o = P_o^{max} \cdot I/I_{max}$. The P_o^{max} values for the individual subunit compositions were determined by single-channel analysis (native channel: 0.82; CNGA2: 0.97; CNGA2B1b: 0.92; CNGA2A4B1b: 0.85) (*10*). To ensure that inhibition rates were not limited by the speed of perfusion change (<50 ms), we analyzed the current decline in Fig. 4 at 500 nM CaM with CNGA2 channels (resulting in $\tau_{fast} > 1$ s) and at 50 nM CaM with CNGA2A4B1b channels (τ_{fast}: 0.8 to 1.3 s).
24. S. E. Gordon, J. Downing-Park, A. L. Zimmermann, *J. Physiol.* **486**, 533 (1995).
25. K.-W. Yau, *Invest. Ophthalmol. Vis. Sci.* **35**, 9 (1994).
26. S. D. Munger *et al.*, *Science* **294**, 2172 (2001).
27. S. Frings, J. Lynch, B. Lindemann, *J. Gen. Physiol.* **100**, 45 (1992)
28. V. Hagen *et al.*, *Angew. Chem. Int. Ed.* **40**, 1046 (2001).
29. V. Hagen *et al.*, *Biochemistry* **35**, 7762 (1996).
30. F. Müller, W. Bönigk, F. Sesti, S. Frings, *J. Neurosci.* **18**, 164 (1998).

31. We thank P. Ascher, B. Barbour, P. Bauer, A. Baumann, F. Müller, and K.-W. Yau for fruitful discussions. We are grateful to V. Hagen for supplying the caged compounds. This work was supported by grants from the Deutsche Forschungsgemeinschaft (SPP 1025), European Community (Bio 4 CT 98 0034), and CNRS (CNRS UMR 8544).

13 June 2001; accepted 28 September 2001